

Detection of Stellar-like Abundance Anomalies in the Slow Solar Wind

David H. Brooks, Deborah Baker, Lidia van Driel-Gesztelyi, Harry P. Warren, Stephanie L. Yardley

▶ **To cite this version:**

David H. Brooks, Deborah Baker, Lidia van Driel-Gesztelyi, Harry P. Warren, Stephanie L. Yardley. Detection of Stellar-like Abundance Anomalies in the Slow Solar Wind. The Astrophysical journal letters, 2022, 930, 10.3847/2041-8213/ac6878 . insu-03713322

HAL Id: insu-03713322
https://insu.hal.science/insu-03713322

Submitted on 4 Jul 2022

HAL is a multi-disciplinary open access archive for the deposit and dissemination of scientific research documents, whether they are published or not. The documents may come from teaching and research institutions in France or abroad, or from public or private research centers.

L'archive ouverte pluridisciplinaire **HAL**, est destinée au dépôt et à la diffusion de documents scientifiques de niveau recherche, publiés ou non, émanant des établissements d'enseignement et de recherche français ou étrangers, des laboratoires publics ou privés.



Distributed under a Creative Commons Attribution 4.0 International License

The Astrophysical Journal Letters, 930:L10 (7pp), 2022 May 1 https://doi.org/10.3847/2041-8213/ac6878
© 2022. The Author(s). Published by the American Astronomical Society.
OPEN ACCESS

Detection of Stellar-like Abundance Anomalies in the Slow Solar Wind

David H. Brooks[1], Deborah Baker[2], Lidia van Driel-Gesztelyi[2,3,4], Harry P. Warren[5], and Stephanie L. Yardley[2]
[1] College of Science, George Mason University, 4400 University Drive, Fairfax, VA 22030, USA
[2] University College London, Mullard Space Science Laboratory, Holmbury St. Mary, Dorking, Surrey, RH5 6NT, UK
[3] LESIA, Observatoire de Paris, Université PSL, CNRS, Sorbonne Université, Univ. Paris Diderot, Sorbonne Paris Cité, 5 place Jules Janssen, F-92195 Meudon, France
[4] Konkoly Observatory, Research Centre for Astronomy and Earth Sciences, Konkoly Thege út 15-17, H-1121, Budapest, Hungary
[5] Space Science Division, Naval Research Laboratory, Washington, DC 20375, USA
Received 2022 March 24; revised 2022 April 18; accepted 2022 April 19; published 2022 May 4

Abstract

The elemental composition of the Sun's hot atmosphere, the corona, shows a distinctive pattern that is different from the underlying surface or photosphere. Elements that are easy to ionize in the chromosphere are enhanced in abundance in the corona compared to their photospheric values. A similar pattern of behavior is often observed in the slow-speed (<500 km s^{-1}) solar wind and in solar-like stellar coronae, while a reversed effect is seen in M dwarfs. Studies of the inverse effect have been hampered in the past because only unresolved (point-source) spectroscopic data were available for these stellar targets. Here we report the discovery of several inverse events observed in situ in the slow solar wind using particle-counting techniques. These very rare events all occur during periods of high solar activity that mimic conditions more widespread on M dwarfs. The detections allow a new way of connecting the slow wind to its solar source and are broadly consistent with theoretical models of abundance variations due to chromospheric fast-mode waves with amplitudes of 8–10 km s^{-1}, sufficient to accelerate the solar wind. The results imply that M-dwarf winds are dominated by plasma depleted in easily ionized elements and lend credence to previous spectroscopic measurements.

Unified Astronomy Thesaurus concepts: Slow solar wind (1873); Solar abundances (1474); Stellar abundances (1577); Solar corona (1483)

1. Introduction

The enhancement of low first-ionization potential (FIP; less than ∼10 eV) elements by factors of 2–4 in the solar corona has become known as the FIP effect (Pottasch 1963; Feldman 1992). A combination of remote-sensing (spectroscopic) measurements of abundances in the solar atmosphere and in situ (particle-counting) measurements in the solar wind has led to a vast literature describing elemental composition in different solar structures (Feldman & Laming 2000), their temporal behavior in different features and dynamic events (Sheeley 1995; Widing 1997; Warren et al. 2016), their use as tracers of a connection to the solar wind (Brooks & Warren 2011; Brooks et al. 2015) or solar energetic particles (Brooks & Yardley 2021), and the development of theoretical models of abundance anomalies (Laming 2004). These studies are complemented by measurements in the range of conditions observed in the coronae of low-activity solar-like stars (Drake et al. 1997).

An inverse FIP (IFIP) effect was detected as a depletion of Fe in the coronae of active stars compared to their photospheres in observations made by the Advanced Satellite for Cosmology and Astrophysics (ASCA) and the Extreme UltraViolet Explorer (EUVE); see Antunes et al. (1994), Stern et al. (1995), Rucinski et al. (1995), Schmitt et al. (1996), and further references in the review by Drake (2002). For a discussion of more recent observations of the IFIP effect, see also Liefke et al. (2008), Wood & Linsky (2010), and Testa et al. (2015). Furthermore, the IFIP effect was recently shown to be present also on stars with higher surface temperatures, if they have evolved off the main sequence and have some indicators of magnetic activity, e.g., a high rotation rate or X-ray luminosity (Seli et al. 2022). But studies of the IFIP effect are relatively less developed because until recently it had only been observed on unresolved stellar targets. In 2015, however, the IFIP effect was discovered on the Sun (Doschek et al. 2015), associated with sunspots during solar flares, allowing the first detailed studies of the process at high spatial and temporal resolution. One possibility is that the IFIP effect observed in M dwarfs is due to enhanced levels of flaring activity. The effect is present in their coronae all the time, however, even when they are not flaring, or at least not producing large flares. Furthermore, observations of elemental abundance changes during flares on several stars that have an IFIP composition or metal-depleted coronae show that the plasma composition evolves toward photospheric during the event (Stern et al. 1992; Mewe et al. 1997; Güdel et al. 1999; Liefke et al. 2010). This is consistent with the new solar observations, which suggest that IFIP-composition plasma is present in cases where, in the presence of emerging flux, magnetically complex sunspots collide, and the flare only acts to reveal (not cause) it by producing high temperatures (Baker et al. 2020). Highly magnetically complex regions are more likely to exist, and dominate the emission, on the more active solar-like stars.

The number of IFIP events so far detected remotely on the Sun is small, and they are all associated with solar flares (Doschek & Warren 2016; Katsuda et al. 2020). Flares are relatively rare in the sense that they are often short duration and occur infrequently. Unlike sampling the constant flow of solar wind, therefore, it would be challenging to observe any signatures of IFIP events in situ. It is not established, however,

Original content from this work may be used under the terms of the Creative Commons Attribution 4.0 licence. Any further distribution of this work must maintain attribution to the author(s) and the title of the work, journal citation and DOI.

that flares are the only source of IFIP composition. We conjectured, therefore, that if the plasma can escape into the heliosphere and form part of the solar wind (an unknown), it might be possible to detect it in situ if an appropriate instrument fortuitously crosses the appropriate solar wind stream at the right time. It has been pointed out (H. Peter 2018, private communication) that a lack of IFIP detection in the solar wind casts some doubt on the reality of the solar IFIP effect, so we felt it worthwhile to pursue. Our best chance would be at a time when potentially more IFIP-composition plasma is being produced, and based on the initial solar observations, this would be most likely at times of extreme magnetic complexity and high activity.

Here we report observations of three IFIP events in situ in the solar wind by the Solar Wind Ion Composition Spectrometer (SWICS; Gloeckler et al. 1998) on the ACE Observatory (Stone et al. 1998).

2. Data and Method

The ACE observations we analyze are SWICS 1.1 level 2 version 4.09 and SWICS 2.0 level 3 version 1.1 data (Shearer et al. 2014), and MAG (Magnetometer) level 2 data that we downloaded from the ACE Science Center at Caltech. We felt that examining a low-/high-FIP element ratio that shows a large variation in the solar wind would give us the best chance of detecting IFIP events. We therefore focused on the Fe/O ratio because Fe and O have a large separation in FIP. We normalized the SWICS data to the photospheric Fe/O abundance ratio of Asplund et al. (2009) (Fe = 7.50; O = 8.69; Fe/O = 0.0646). The mean error for the absolute Fe/O abundance ratios in the data set is less than 2%. These are the statistical uncertainties due to limited count statistics provided by the SWICS team. They do not include any source of systematic error. Such errors can arise from several sources, for example, misidentification of ions, uncertainties in the geometric sensitivity of the instrument, etc. von Steiger & Zurbuchen (2011) made an assessment of these error sources and argued that the impact on relative abundance measurements, like Fe/O, is not too large (less than 10% for the largest factor: detector efficiency—see their Table A1). When searching the database, we identified IFIP events if the normalized abundance ratio was 30% lower than the photospheric abundance ratio. Compared to the estimates of statistical and systematic uncertainties, a 30% decrease is significant. We chose this relatively large threshold for detection in order to find the most significant events and also to compensate for the fact that there is a spread in photospheric Fe/O abundance ratios in the recent literature from 0.0575–0.0646 (Asplund et al. 2009; Caffau et al. 2011; Scott et al. 2015). Under these conditions, the IFIP events are detected regardless of which of these sources is used for the photospheric abundances; larger variations are seen in earlier data sets (see discussion below), but we restrict ourselves to these recent compilations.

We first searched the SWICS daily database between 1998 February 4 and the hardware problem on 2011 August 23. We show a histogram of all the values during this time period in Figure 1. The histogram peaks at a normalized Fe/O photospheric value of 2.1 and the standard deviation is 0.7—assuming a normal distribution. Our IFIP event detection threshold therefore roughly corresponds to a confidence level of ∼95% (i.e., 2σ). The distribution, however, is in fact

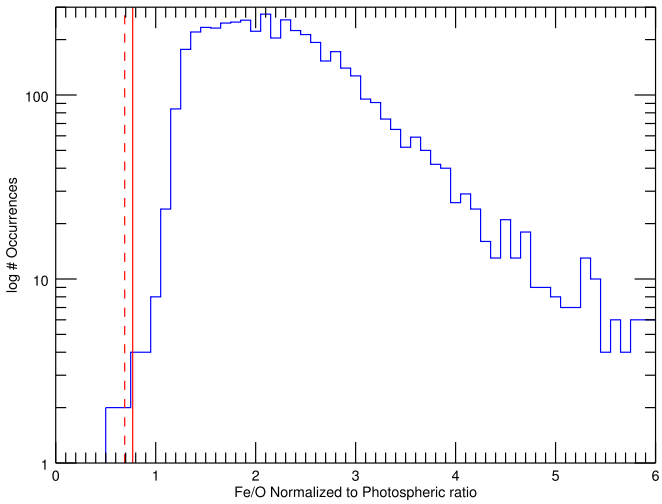


Figure 1. ACE/SWICS measurements of Fe/O normalized to their photospheric ratio. The data were obtained between 1998 February and 2011 August. The red solid line indicates the level we have defined for IFIP detection. Whether the measurements fall below this level depends on the assumed photospheric Fe/O abundance, and these vary in the literature, so for reference, we also show the threshold that would need to be reached if a more extreme lower value is chosen (see Section 2).

right-hand-skewed to higher values, implying that the standard deviation assuming a normal distribution is overestimated so the statistical significance of the detections will be underestimated. The initial search found anomalies on five separate occasions in the daily database. As can be seen in Figure 1, these are very rare events. It is worth noting that even photospheric Fe/O ratios are rare in this data set. Because we define an IFIP detection as 30% below photospheric Fe/O values, it makes sense to define photospheric Fe/O ratios as 1 ± 0.3. Analyzing the skewed distribution, we find that $<10\%$ of the values are photospheric events. When IFIP events were detected, we then downloaded the more detailed 2-hourly data, but we were only able to confirm the presence of three events in the 2-hourly data. We also examined the SWICS 2-hourly data post-2011 but found no anomalies in that time period. In all the cases that were detected, the data quality is poor at some stage during or after the event, so the exact durations are difficult to determine. In several cases, the measurements are flagged as having data missing from the velocity distribution functions (VDF). In some cases, the VDFs are completely empty, whereas in other cases the data are flagged as being marginally valid. We excluded all data that were not flagged as clean. In SWICS data, larger uncertainties can also occur due to low count rates, which suggest a depletion of the low-FIP element Fe. Whether low-FIP elements are depleted or high-FIP elements are enhanced during the IFIP effect is another topic of interest. The ponderomotive force model due to Laming (2004) suggests the FIP and IFIP effects act solely on low-FIP elements, and there is some evidence in support of this from observations by the EUV Imaging Spectrometer on the Hinode satellite (Brooks 2018). The SWICS measurements we report here are in agreement with that scenario. If the high-FIP element O were enhanced, we would be less likely to encounter difficulties due to low count rates.

There were multiple numbered active regions on disk during the IFIP events; including several extremely large ones. For each IFIP event, we also discuss the potential source region and its coronal magnetic field topology using data obtained by the

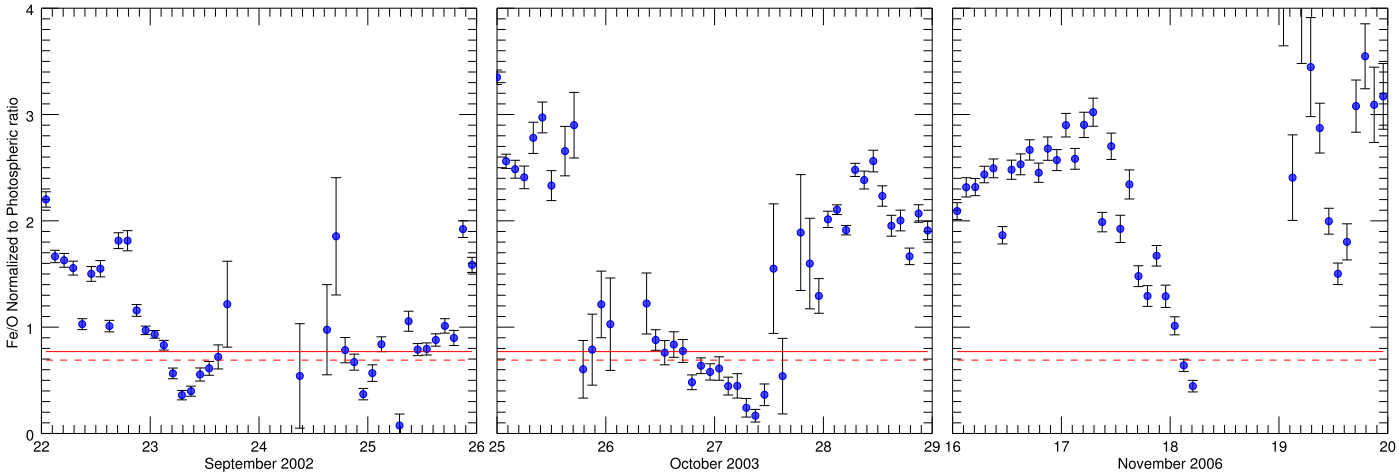


Figure 2. IFIP events detected in the solar wind by ACE/SWICS. Fe/O abundance ratios measured by SWICS in situ in the solar wind normalized to their photospheric abundance ratio. Measurement uncertainties are shown by the error bars. The red solid and dashed lines correspond to the same levels as shown in Figure 1. We removed all data flagged as poor/marginal quality or missing due to numerical errors, low statistics, or anomalous operations.

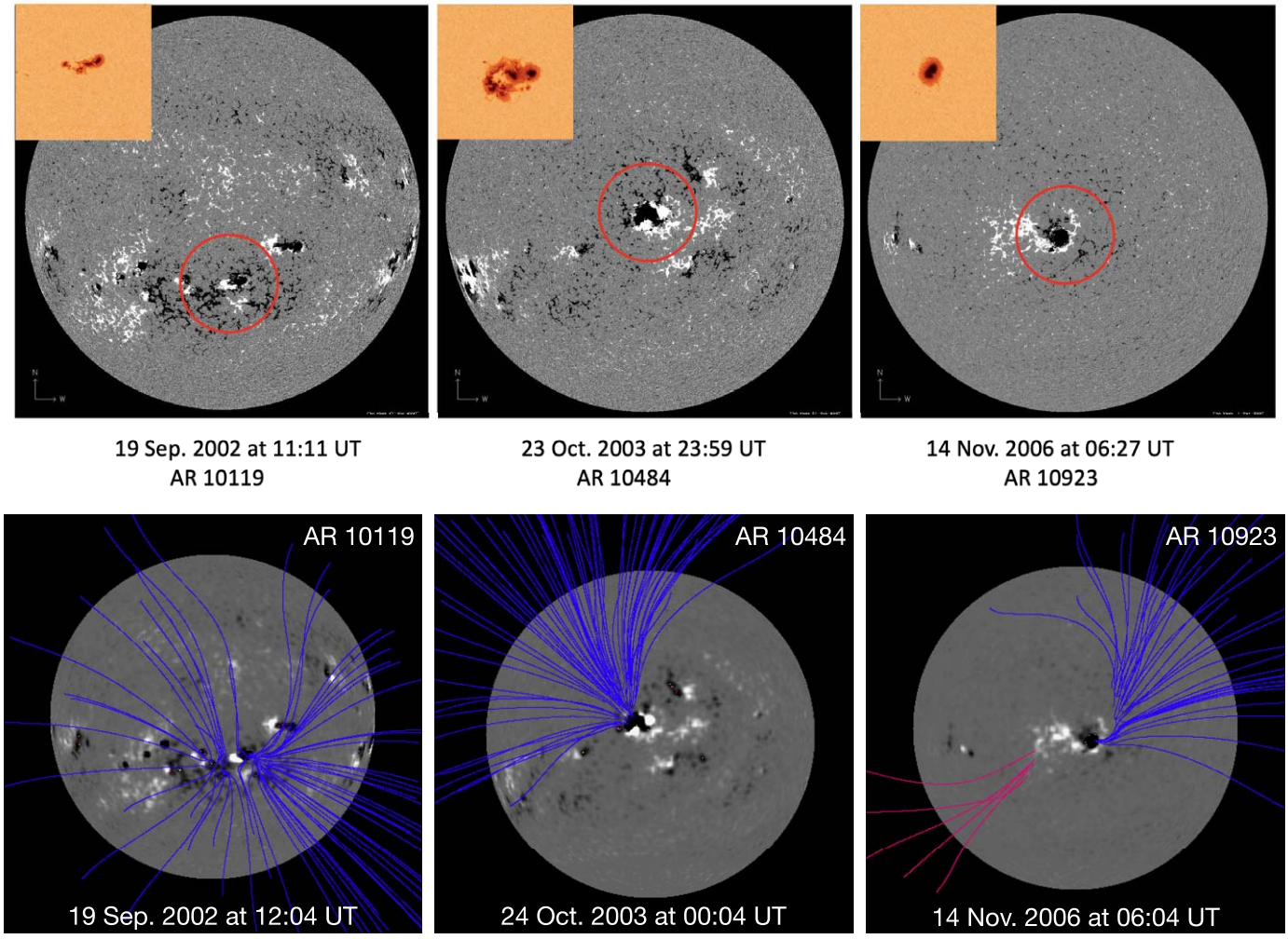


Figure 3. Top panels: SOHO/MDI full solar disk magnetograms with accompanying photospheric continuum images (colored insets). We show the longitudinal magnetic field in the solar photosphere at the times of the likely departure of the back-mapped solar wind of the events in 2002, 2003, and 2006, with the red circles indicating the likely source regions. These images highlight the complexity of the magnetic field on the Sun during the IFIP events. White indicates positive polarity, and black indicates negative polarity. The images are scaled from −500 to 500 G. Bottom panels: open coronal magnetic field lines taken from the PFSS model for each active region (AR 10119, 10484, and 10923). The blue field lines indicate negative polarity, and the pink field lines represent positive polarity magnetic field. The grayscale images are reduced-resolution MDI full-disk observations of the longitudinal magnetic field in the solar photosphere with white showing positive polarity and black showing negative polarity, scaled from −200 to 200 G.

Michelson Doppler Imager (MDI; Scherrer et al. 1995) on the Solar and Heliospheric Observatory (SOHO; Domingo et al. 1995). We used full-disk observations of the longitudinal (line-of-sight) magnetic field in the solar photosphere. The data were downloaded from the Joint Science Operations Center (JSOC) at Stanford via the Virtual Solar Observatory gateway and have been calibrated with the best available methods. To examine the coronal magnetic field topology we used potential field source surface (PFSS) models (Schatten et al. 1969). For each time period of interest, we generated PFSS extrapolations using the package available in SolarSoftware (Schrijver & De Rosa 2003). This package accesses a database of potential field models constructed from the MDI photospheric magnetic field data. Field lines are traced out from the solar surface with those reaching the source surface designated as open.

3. Results and Discussion

The three events we describe occurred in 2002 September, 2003 October, and 2006 November. We show the Fe/O abundance ratios, normalized to their photospheric ratios, in Figure 2, and full-disk images of the longitudinal magnetic field at the back-mapped time of these detections in Figure 3 along with potential field extrapolations indicating the locations of the open magnetic field at the times of the likely departure of the solar wind (back-mapped using the ACE-measured speed). The figure highlights the three potential active region sources of the events we detected (AR 10119, 10484, and 10923), and we highlight the extrapolated open field lines connected to these regions.

The clearest and most significant event we found occurred on 2003 October 26–27. This was during the famous Halloween storms, when numerous major flares (>M5 class) occurred between October 19 and November 20, including 4 of the 10 strongest X-class flares recorded this century, and the most powerful (X45) flare of the space age, although the source region of the most intense flares was AR 10486 not AR 10484, which, however, also produced a few X-class and several M-class flares. The Fe/O ratio also reached record highs during this period, so solar conditions were at their most extreme in the days surrounding the time of this event. The Fe/O ratio dropped below photospheric levels from ∼11 UT on the 26th and recovered to nominal values some time after 11 UT on the 27th. The event was therefore sustained for around 24 hr.

The 2002 September event was also potentially of long duration but was less clear. The Fe/O ratio dropped below photospheric levels around 23 UT on the 22nd, but only reached values significant enough for our detection (see Section 2) around 5 UT on the 23rd. The data are highly uncertain or missing between 17 UT on the 23rd and 19 UT on the 24th before IFIP composition is detected again until ∼1 UT on the 25th and photospheric composition thereafter. It is unclear whether the two detections are part of the same event, but they were also associated with high solar activity. Two M-class flares occurred a few days before, and there were an unusually large number of active regions (⩾15) on disk at the solar wind velocity back-mapped time (see Figure 3).

The 2006 November event was only detected for a short duration. A normal FIP effect was observed in the solar wind one day prior to the event, but the Fe/O ratio trended downward over the preceding 24 hr and hit subphotospheric levels for 2–6 hr around 4 UT on the 18th. The data are highly uncertain after that time, but if this is due to low count rates for Fe, then it is plausible that this event was also long duration. Flaring activity was not significant during this event, but, at the back-mapped time, there was an active region with a very large leading spot in the middle of the solar disk (see Figure 3). The average magnitude of the IFIP effect is about a factor of 2 in these three examples.

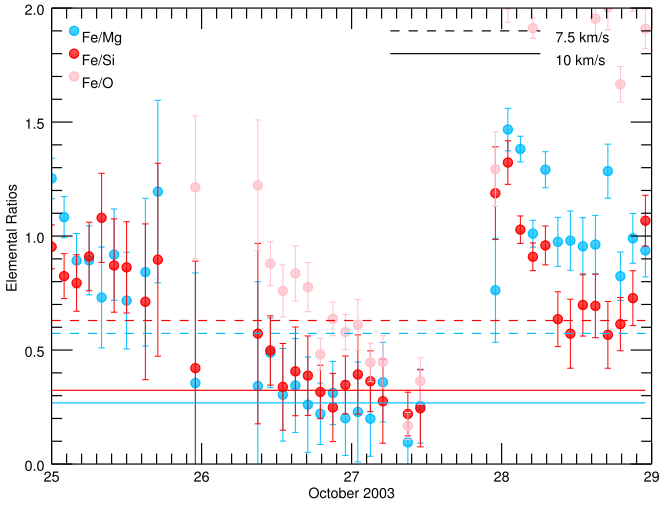


Figure 4. Elemental abundance ratios compared to the ponderomotive force model. Fe/O, Fe/Si, and Fe/Mg abundance ratios measured by SWICS in situ in the solar wind during the 2003 October IFIP event and normalized to their photospheric abundance ratios. We compare the measurements to theoretical values predicted from the ponderomotive force model of IFIP due to Laming (2015). We show the theoretical predictions for two different values of the fast-mode wave amplitude in the models. Measurement uncertainties are shown by the error bars.

There may be other ways that similar events could be detected in the solar wind. We searched the literature for older observations and found some interesting historical evidence in support of these detections from SOHO/CELIAS. Aellig et al. (1999) studied the Fe/O abundance ratio over an 80 day period near solar minimum in 1996, 1996 June ∼1–1996 August 19, and show distributions of values for different wind speeds extending down to photospheric abundances (∼1.4 in their Figure 3, which shows log Fe/O ratios). At the time of their calculations, however, the accepted photospheric Fe/O abundance ratio dated back to 1989 (Anders & Grevesse 1989) and is a factor of 1.8 lower than recent estimates from the same group (Asplund et al. 2009). This means that the tail of the distribution of Fe/O ratios for the slow wind (<360 km s^{-1}) in the CELIAS data, for example, is showing an IFIP effect of a factor of 2, albeit this part of the distribution also represents rare cases.

One potentially very important consequence of the detection of these events in the solar wind is that they allow new examination of the properties of MHD waves that can heat and accelerate the solar wind, using other in situ measurements. In Figure 4 we make an initial comparison of the SWICS observations from 2003 October with the ponderomotive force model of the IFIP effect (Laming 2015). In this model, chromospheric acoustic waves propagating from below, mode convert to become fast-mode waves that then reflect downward. This leads to a downward-directed ponderomotive force that depletes the region of low-FIP elements. We show the SWICS Fe/O, Fe/Si, and Fe/Mg abundance ratios during this event plotted against the predicted ratios from the IFIP effect model. The predictions are made based on different values of

the fast-mode wave amplitude at the layer where magnetic and plasma pressure is approximately equal. The observed results are broadly consistent with fast-mode wave amplitudes of 7.5–10 km s^{-1} for all three events. These values are similar to the lower end of wave amplitudes measured previously in the chromosphere and corona but are still strong enough to accelerate the solar wind if the energy flux transmission coefficient is high enough (De Pontieu et al. 2007).

Using another in situ measurement we also show that all three IFIP events are detected in the slow solar wind. Figure 5 (top panel) shows the bulk solar wind speed in the time periods covering these detections. In all cases, the wind speed is below ~600 km s^{-1} in the days preceding the events, while the plasma traveled to the L1 Lagrange point. The origin of the slow solar wind is still under debate, and active regions have been suggested as one possible source (Liewer et al. 2004). There is a difficulty, however, in using plasma composition measurements to definitively identify the sources. This is because an enhanced slow-wind composition may be observed in multiple active regions on the solar disk at the same time, and even in different features such as coronal loops and outflows within the same active region (Brooks & Warren 2011). The discovery of IFIP-composition plasma in the slow wind implies that specific magnetically complex areas that produce this within active regions can also be slow solar wind sources. To be clear, solar observations have thus far only detected IFIP-composition plasma above sunspots in complex flaring regions. Our observations indicate that complex sunspots are a previously unrecognized source of slow solar wind.

Our ACE-measured solar wind speed back-mapped times, however, all single out one respective active region as the most likely source of the IFIP-composition slow solar wind. All three active regions have open field lines, the magnetic polarities of which match the polarities of the slow wind where the IFIP composition was detected (as we show in Figure 5—middle panel). The figure shows the interplanetary magnetic field direction, B_x in Geocentric Solar Ecliptic (GSE) coordinates, measured by ACE/MAG. The data are plotted on a common timescale as in the upper panel. For the 2002 September event (sky blue dots), B_x is always positive, i.e., directed sunward, which matches the negative polarity (opposite convention) of the open magnetic field observed in the active region. For the 2003 October event, B_x is initially negative but has turned positive by the time the IFIP effect is detected. The 2006 November measurements are more variable, with B_x spreading positive and negative values as the FIP bias trends downward (November 17; day 1 in Figure 5) but is again predominantly positive when the IFIP effect is detected (November 18; day 2 in Figure 5).

Only one of the three active regions (AR 10484), however, is a highly complex emerging AR similar to those in which IFIP composition was detected previously (Baker et al. 2020). The second potential source region is a medium-sized active region (AR 10119), which was in its emergence phase when it was linked to IFIP-composition solar wind. The third active region (AR 10923) has its large decaying leading spot to make it stand out. These two latter active regions broaden the class of solar active regions that can produce IFIP coronal plasma composition to cases that are less unusual. This indicates that localized IFIP production in active regions may be more common than previously thought. Active regions with high magnetic flux

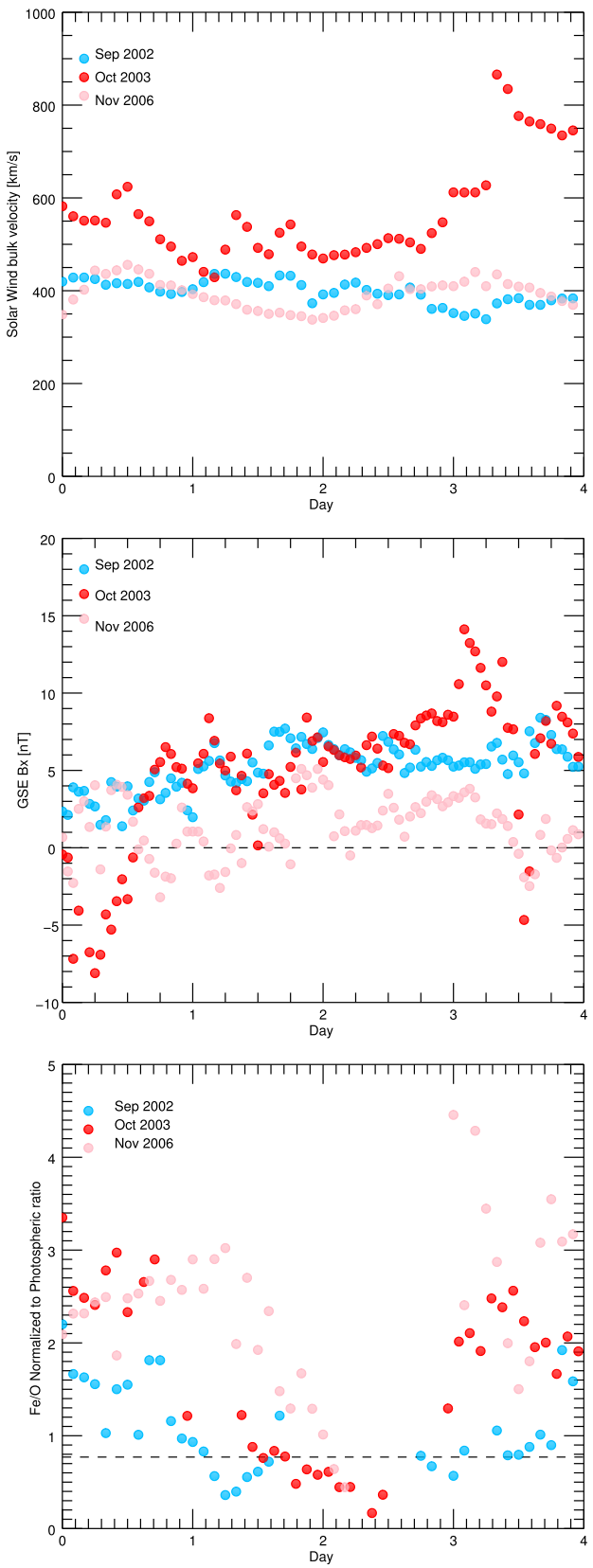


Figure 5. Solar wind velocity, interplanetary magnetic field direction, and Fe/O ratios during the IFIP events. Top panel: He++ velocity measured by SWICS in situ around the time period of the three IFIP events shown in Figure 2. Middle panel: B_x measured by ACE/MAG in situ around the time period of the three IFIP events shown in Figure 2. Bottom panel: the three IFIP events in Figure 2 plotted for ease of cross-reference. We show all the data on a common timescale that corresponds to the ranges in Figure 2.

density in their emergence phase may be good candidates for IFIP plasma production. Observing clear signals of this in the slow solar wind would be an unlikely event, however, because a number of conditions would have to be met. For example, there must be open magnetic fields in the vicinity of the sunspot umbra where the usually highly localized IFIP plasma is observed—or an alternative escape pathway. Furthermore, the IFIP-composition plasma may be localized within the active region embedded in a coronal composition-dominated environment, so plasma mixing with surrounding coronal composition material as the solar wind forms may dilute the signature and mask most of these events before they reach the observing spacecraft. Because these events are also of relatively short duration (compared to the active region lifetime), there is a reduced chance of it being at the footpoint of the slow-wind stream that connects to the spacecraft, which is itself a low-probability event.

The rarity of the IFIP events of course implies that their source is only a very minor contributor to the slow solar wind. They are potentially very valuable, however, for remote sensing and in situ connection modeling, precisely because they are rare and localized to specific regions. The detections by SWICS suggest that future missions such as Solar Orbiter may also observe IFIP events, and it may be easier to link these to specific footpoints of the wind connecting to the spacecraft because there may be only one location producing IFIP-composition plasma. Very detailed observations of the source region will then become possible, allowing refinement of the model predictions that are currently used.

The discovery of these events also confirms that IFIP-composition plasma can escape into the heliosphere. Although there is no theoretical reason to think otherwise, it is important to stress that this was unknown before the detection and has implications for stellar observations. The fact that there is no impediment to this plasma flowing into the solar wind implies that solar-like stars with IFIP-composition coronae, such as M dwarfs, have stellar winds that are also dominated by IFIP-composition plasma—very different from the Sun. Furthermore, any gradual solar energetic particle (SEP)-like events on these stars will also have an IFIP composition because the seed population comes from the corona, with implications for exoplanet atmospheres.

All the previous spectroscopic results are necessarily dependent on the quality of the underlying atomic physics. In the case of the Sun, only a limited number of specific Ar and Ca spectral lines have been used to detect the IFIP effect, and the particular Ca line (Ca XIV 193.874 Å) has shown unusual width behavior in solar observations (Brooks & Warren 2016). Modeling assumptions, such as ionization equilibrium, also introduce uncertainties. For the M dwarfs, there are generally no measurements of their photospheric abundances (Laming 2015), so the IFIP effect is computed relative to solar photospheric abundances. This means that if their photospheric elemental abundance distributions are different from that of the Sun, as their coronal and apparently now wind compositions appear to be, then the IFIP effect could be smaller or even nonexistent. Our detection of the inverse FIP effect by particle-counting techniques in the solar wind lends support to all the IFIP effect findings by completely different spectroscopic methods.

We thank the anonymous reviewer for several detailed comments and suggestions that improved the manuscript. The work of D.H.B. and H.P.W. was funded by the NASA Hinode program. D.B. is funded under STFC consolidated grant number ST/S000240/1, and L.v.D.G. is partially funded under the same grant. L.v.D.G. acknowledges the Hungarian National Research, Development and Innovation Office grant OTKA K-131508. The work of S.L.Y. was carried out with support from the UKRI SWIMMR Aviation Risk Modeling (SWARM) grant. We thank the ACE SWICS and MAG instrument teams and the ACE Science Center for providing the ACE data.

ORCID iDs

David H. Brooks https://orcid.org/0000-0002-2189-9313
Deborah Baker https://orcid.org/0000-0002-0665-2355
Lidia van Driel-Gesztelyi https://orcid.org/0000-0002-2943-5978
Harry P. Warren https://orcid.org/0000-0001-6102-6851
Stephanie L. Yardley https://orcid.org/0000-0003-2802-4381

References

Aellig, M. R., Hefti, S., Grünwaldt, H., et al. 1999, JGR, 104, 24769
Anders, E., & Grevesse, N. 1989, GeCoA, 53, 197
Antunes, A., Nagase, F., & White, N. E. 1994, ApJL, 436, L83
Asplund, M., Grevesse, N., Sauval, A. J., & Scott, P. 2009, ARA&A, 47, 481
Baker, D., van Driel-Gesztelyi, L., Brooks, D. H., et al. 2020, ApJ, 894, 35
Brooks, D. H. 2018, ApJ, 863, 140
Brooks, D. H., Ugarte-Urra, I., & Warren, H. P. 2015, NatCo, 6, 5947
Brooks, D. H., & Warren, H. P. 2011, ApJL, 727, L13
Brooks, D. H., & Warren, H. P. 2016, ApJ, 820, 63
Brooks, D. H., & Yardley, S. L. 2021, SciA, 7, eabf0068
Caffau, E., Ludwig, H. G., Steffen, M., Freytag, B., & Bonifacio, P. 2011, SoPh, 268, 255
De Pontieu, B., McIntosh, S. W., Carlsson, M., et al. 2007, Sci, 318, 1574
Domingo, V., Fleck, B., & Poland, A. I. 1995, SoPh, 162, 1
Doschek, G. A., & Warren, H. P. 2016, ApJ, 825, 36
Doschek, G. A., Warren, H. P., & Feldman, U. 2015, ApJL, 808, L7
Drake, J. J. 2002, in ASP Conf. Ser. 277, Stellar Coronae in the Chandra and XMM-NEWTON Era, ed. F. Favata & J. J. Drake (San Francisoc, CA: ASP), 75
Drake, J. J., Laming, J. M., & Widing, K. G. 1997, ApJ, 478, 403
Feldman, U. 1992, PhyS, 46, 202
Feldman, U., & Laming, J. M. 2000, PhyS, 61, 222
Gloeckler, G., Cain, J., Ipavich, F. M., et al. 1998, SSRv, 86, 497
Güdel, M., Linsky, J. L., Brown, A., & Nagase, F. 1999, ApJ, 511, 405
Katsuda, S., Ohno, M., Mori, K., et al. 2020, ApJ, 891, 126
Laming, J. M. 2004, ApJ, 614, 1063
Laming, J. M. 2015, LRSP, 12, 2
Liefke, C., Fuhrmeister, B., & Schmitt, J. H. M. M. 2010, A&A, 514, A94
Liefke, C., Ness, J. U., Schmitt, J. H. M. M., & Maggio, A. 2008, A&A, 491, 859
Liewer, P. C., Neugebauer, M., & Zurbuchen, T. 2004, SoPh, 223, 209
Mewe, R., Kaastra, J. S., van den Oord, G. H. J., Vink, J., & Tawara, Y. 1997, A&A, 320, 147
Meyer, J. P. 1985, ApJS, 57, 173
Pottasch, S. R. 1963, ApJ, 137, 945
Rucinski, S. M., Mewe, R., Kaastra, J. S., Vilhu, O., & White, S. M. 1995, ApJ, 449, 900
Schatten, K. H., Wilcox, J. M., & Ness, N. F. 1969, SoPh, 6, 442
Scherrer, P. H., Bogart, R. S., Bush, R. I., et al. 1995, SoPh, 162, 129
Schmitt, J. H. M. M., Stern, R. A., Drake, J. J., & Kuerster, M. 1996, ApJ, 464, 898
Schrijver, C. J., & De Rosa, M. L. 2003, SoPh, 212, 165
Scott, P., Grevesse, N., Asplund, M., et al. 2015, A&A, 573, A25
Seli, B., Oláh, K., Kriskovics, L., et al. 2022, A&A, 659, A3
Shearer, P., von Steiger, R., Raines, J. M., et al. 2014, ApJ, 789, 60
Sheeley, N. R. J. 1995, ApJ, 440, 884
Stern, R. A., Lemen, J. R., Schmitt, J. H. M. M., & Pye, J. P. 1995, ApJL, 444, L45

Stern, R. A., Uchida, Y., Tsuneta, S., & Nagase, F. 1992, ApJ, 400, 321
Stone, E. C., Frandsen, A. M., Mewaldt, R. A., et al. 1998, SSRv, 86, 1
Testa, P., Saar, S. H., & Drake, J. J. 2015, RSPTA, 373, 20140259
von Steiger, R., & Zurbuchen, T. H. 2011, JGRA, 116, A01105
Warren, H. P., Brooks, D. H., Doschek, G. A., & Feldman, U. 2016, ApJ, 824, 56
Widing, K. G. 1997, ApJ, 480, 400
Wood, B. E., & Linsky, J. L. 2010, ApJ, 717, 1279